Journal of Guidance, Control, and Dynamics, Vol. 43, No. 10, 2020, pp. 1935–1942. doi: http://doi.org/10.2514/1.G005193

Solar Sail Optimal Transfer Between Heliostationary Points

Alessandro A. Quarta,* Giovanni Mengali,† Lorenzo Niccolai‡
Department of Civil and Industrial Engineering, University of Pisa, I-56122 Pisa, Italy

Nomenclature

$\boldsymbol{a}$	=	propulsive acceleration vector, mm/s^2
a_r, a_θ	=	propulsive acceleration components, mm/s^2
$\mathcal{E}$	=	dimensionless error
$\mathcal{F}$	=	auxiliary function, see Eq. (17)
$\mathcal{H}$	=	Hamiltonian function
h	=	specific angular momentum magnitude, km^2/s
J	=	performance index, days
$\hat{\boldsymbol{n}}$	=	normal unit vector in the direction opposite to the Sun
O	=	Sun's center of mass
$\mathcal{P}$	=	reference plane
$\hat{\boldsymbol{r}}$	=	position unit vector
r	=	Sun-spacecraft distance, km
$\mathcal{T}$	=	polar reference frame
t	=	time, days
u	=	radial component of velocity, km/s
α	=	cone angle, rad
β	=	sail lightness number
θ	=	spacecraft polar angle, rad
$\{\lambda_r, \lambda_\theta, \lambda_u, \lambda_h\}$	=	adjoint variables
$\mu_\odot$	=	Sun's gravitational parameter, km^3/s^2

Subscripts

0	=	initial value
1	=	at perihelion
f	=	final (target) value
min	=	minimum

Superscripts

$\cdot$	=	time derivative
$\wedge$	=	unit vector

Introduction

A notable feature of propellantless propulsion systems such as solar sails [1,2] is in their capability of generating a continuous thrust for a long time span, theoretically limited only by the degradation of the sail film material [3–5]. This allows advanced mission scenarios [6] to be conceived, which would be impossible to design with conventional propulsive systems [7, 8].

In this respect, a challenging space mission consists in the maintenance of a heliostationary point, that is, a static equilibrium in a heliocentric inertial reference frame [9, 10]. When placed in a heliostationary condition, the spacecraft has zero inertial velocity, and its propulsive acceleration must balance the Sun's gravitational attraction. The maintenance of a heliostationary point requires the spacecraft to be propelled by a high-performance solar sail, of which the characteristic acceleration [11] is still beyond the current technological capabilities. More precisely, the sail propulsive acceleration necessary for maintaining a heliostationary point is similar to that required to perform a H-reversal trajectory [12], or a Solar System escape via a photonic gravity assist [13]. The peculiarities of heliostationary points make them good candidates for future scientific mission concepts, such as the continuous monitoring of solar poles, or the release of a small solar probe, of which the aim is to fall freely to the Sun [14] to obtain in-situ information about corona and solar wind characteristics . These aspects have promoted the analysis of solar sail dynamics in the vicinity of a heliostationary point, which started from the pioneering work by Dandouras et al. [14], and has encouraged the study of possible applications for other (propellantless) propulsion systems [15].

This Note analyzes the transfer between two heliostationary points having the same distance from the Sun. The problem is addressed within an optimal framework in which a constraint is enforced on the minimum Sun-spacecraft distance along the transfer trajectory. A relevant contribution of this Note consists of the development of an approximate model, which allows the time-optimal transfer between two heliostationary points (having the same distance from the Sun) to be found with an

*Professor, a.quarta@ing.unipi.it. Associate Fellow AIAA (**corresponding author**).
†Professor, g.mengali@ing.unipi.it. Senior Member AIAA.
‡Research assistant, lorenzo.niccolai@ing.unipi.it

analytical solution. The latter is accurate enough for a preliminary mission design phase, as long as the angular displacement between the two heliostationary points does not exceed some tens degrees. In addition, the closed-form expression of the optimal control law gives interesting insights into the actual (nonlinear) optimal transfer problem, and allows the designer to obtain an accurate guess of the unknown initial costates when an indirect approach is used to solve the optimization problem.

Problem description

Consider the heliocentric motion of a solar sail-based spacecraft and assume its propulsive acceleration $\boldsymbol{a}$ (i.e., the acceleration due to the solar sail) to be described by an ideal force model as [16]

$$\boldsymbol{a} = \beta \, \frac{\mu_\odot}{r^2} \, \cos^2 \alpha \, \hat{\boldsymbol{n}} \tag{1}$$

where $\mu_\odot$ is the Sun's gravitational parameter, r is the Sun-spacecraft distance, $\hat{\boldsymbol{n}}$ is the unit vector normal to the sail nominal plane in the direction opposite to the Sun, and α is the sail cone angle, that is, the angle between the unit vector $\hat{\boldsymbol{r}}$ (parallel to the Sun-spacecraft line) and $\hat{\boldsymbol{n}}$, with $\cos\alpha = \hat{\boldsymbol{n}} \cdot \hat{\boldsymbol{r}}$. In Eq. (1), β is the sail lightness number [11], defined as the ratio of the maximum propulsive acceleration magnitude (i.e., the value of $\|\boldsymbol{a}\|$ when $\alpha = 0$) to the local solar gravitational acceleration. At time $t_0 \triangleq 0$ the spacecraft is in an equilibrium (heliostationary) condition at a given solar distance r_0, where the spacecraft inertial velocity is zero and the sail propulsive acceleration balances the Sun's gravitational pull. Its initial propulsive acceleration is therefore $\boldsymbol{a}_0 \triangleq \boldsymbol{a}(t_0) = (\mu_\odot / r_0^2) \hat{\boldsymbol{r}}_0$ with $\hat{\boldsymbol{r}}_0 \equiv \hat{\boldsymbol{r}}(t_0)$, see Eq. (1) when $r = r_0$, $\beta = 1$, $\alpha = 0$ and $\hat{\boldsymbol{n}} = \hat{\boldsymbol{r}}_0$.

The problem discussed in this Note is to minimize the time t_f required to transfer the spacecraft from an initial heliostationary position, defined by the vector $\boldsymbol{r}_0 = r_0 \, \hat{\boldsymbol{r}}_0$, to a final heliostationary position at the same heliocentric distance, that is, $\boldsymbol{r}_f = r_0 \, \hat{\boldsymbol{r}}_f$ with $\hat{\boldsymbol{r}}_f \neq \hat{\boldsymbol{r}}_0$; see Fig. 1.

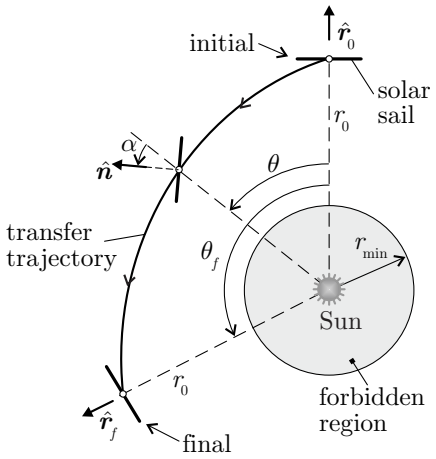

Figure 1 Conceptual sketch of the mission scenario.

The transfer trajectory may be analyzed within a two-dimensional framework, by considering the reference plane $\mathcal{P}$ that contains the two unit vectors $\hat{\boldsymbol{r}}_0$ and $\hat{\boldsymbol{r}}_f$. In the special case when $\hat{\boldsymbol{r}}_f = -\hat{\boldsymbol{r}}_0$, $\mathcal{P}$ is any fixed plane that contains the initial Sun-spacecraft line. The spacecraft dynamics can be conveniently described using a polar reference frame $\mathcal{T}(O; r, \theta)$, of which the origin O is the Sun's center-of-mass, while $\theta \triangleq \arccos(\hat{\boldsymbol{r}} \cdot \hat{\boldsymbol{r}}_0)$ is the polar angle measured counterclockwise from the initial Sun-spacecraft direction; see Fig. 1. In this scenario, the (single) sail control parameter is the cone angle that ranges in the interval $\alpha \in [-\pi/2, \, \pi/2]$ rad. Note that, because $r_f = r_0$, the problem amounts to minimizing the time necessary to change the spacecraft polar angle θ from $\theta_0 \triangleq \theta(t_0) = 0$ to $\theta_f \triangleq \theta(t_f) \in (0, \, \pi]$ rad, see Fig. 1.

The spacecraft equations of motion in $\mathcal{T}$ are given by

$$\ddot{r} = r \, \dot{\theta}^2 - \frac{\mu_\odot}{r^2} + a_r \quad , \quad \ddot{\theta} = \frac{2 \, \dot{r} \, \dot{\theta} - a_\theta}{r} \tag{2}$$

where a_r (or a_θ) is the radial (or transverse) component of the propulsive acceleration $\boldsymbol{a}$. Bearing in mind that $\beta = 1$, Eq. (1) yields

$$a_r = \frac{\mu_\odot}{r^2} \, \cos\alpha^3 \quad , \quad a_\theta = \frac{\mu_\odot}{r^2} \, \cos\alpha^2 \, \sin\alpha \tag{3}$$

so that Eqs. (2) can be rewritten as a system of four first-order differential equations, viz.

$$\dot{r} = u \quad , \quad \dot{\theta} = \frac{h}{r^2} \quad , \quad \dot{u} = \frac{h^2}{r^3} - \frac{\mu_\odot}{r^2} \left(1 - \cos^3 \alpha \right) \quad , \quad \dot{h} = \frac{\mu_\odot}{r} \cos^2 \alpha \, \sin\alpha \tag{4}$$

with initial conditions

$$r(t_0) = r_0 \quad , \quad \theta(t_0) = 0 \quad , \quad u(t_0) = 0 \quad , \quad h(t_0) = 0 \tag{5}$$

where u is the radial component of the spacecraft velocity, and $h \triangleq r^2 \, \dot{\theta}$ is the spacecraft specific angular momentum magnitude.

The time-optimal variation of the sail cone angle α is obtained by maximizing the performance index $J \triangleq -t_f$ with terminal constraints

$$r(t_f) = r_0 \quad , \quad \theta(t_f) = \theta_f \quad , \quad u(t_f) = 0 \quad , \quad h(t_f) = 0 \tag{6}$$

Preliminary simulations show that the optimal transfer trajectory tends to approach the Sun when θ_f is sufficiently large. Therefore, a path constraint is enforced in the trajectory analysis in the form $r \geq r_{\min}$, where $r_{\min} > 0$ is the minimum admissible value of the Sun-spacecraft distance, imposed by thermal constraints [17]; see Fig. 1.

Trajectory optimization

The optimal performance is calculated with an indirect approach in which the Hamiltonian function $\mathcal{H}$ is a constant of motion [18], given by

$$\mathcal{H} \triangleq \lambda_r\, u + \frac{\lambda_\theta\, h}{r^2} + \frac{\lambda_u\, h^2}{r^3} - \frac{\lambda_u\, \mu_\odot}{r^2}\left(1-\cos^3\alpha\right) + \frac{\lambda_h\, \mu_\odot}{r}\cos^2\alpha\,\sin\alpha \tag{7}$$

where $\{\lambda_r,\, \lambda_\theta,\, \lambda_u,\, \lambda_h\}$ are the adjoint variables associated with the state variables, and α is the only control variable. Using the Euler-Lagrange equations, the time derivatives of the adjoint variables are

$$\begin{aligned} &\dot\lambda_r = \frac{2\,\lambda_\theta\, h}{r^3} + \frac{3\,\lambda_u\, h^2}{r^4} - \frac{2\,\lambda_u\,\mu_\odot}{r^3}\left(1-\cos^3\alpha\right) + \frac{\lambda_h\,\mu_\odot}{r^2}\cos^2\alpha\,\sin\alpha, \\ &\dot\lambda_\theta = 0, \qquad \dot\lambda_u = -\lambda_r, \qquad \dot\lambda_h = -\frac{\lambda_\theta}{r^2} - \frac{2\,\lambda_u\, h}{r^3} \end{aligned} \tag{8}$$

The optimal steering law is found by maximizing the Hamiltonian $\mathcal{H}$, in accordance with Pontryagin's maximum principle. This amounts to maximizing $\mathcal{H}'$, defined as

$$\mathcal{H}' = \frac{\lambda_u\,\mu_\odot}{r^2}\left(1-\cos^3\alpha\right) + \frac{\lambda_h\,\mu_\odot}{r}\cos^2\alpha\,\sin\alpha \tag{9}$$

which denotes the part of the Hamiltonian that is function of the control variable α. The required value of α may be written as a function of the two adjoint variables $\{\lambda_u,\, \lambda_h\}$, by adapting the classical result by Sauer [19], viz.

$$\alpha = \arctan\left(\frac{-3\,\lambda_u + \sqrt{9\,\lambda_u^2 + 8\lambda_h^2\, r^2}}{4\,\lambda_h\, r}\right) \tag{10}$$

In particular, Eq. (10) coincides with the solution of the necessary condition $\partial\mathcal{H}'/\partial\alpha = 0$.

The two-point boundary value problem (2PBVP) associated with the optimal transfer with no path constraint (that is, without constraints on the minimum Sun-spacecraft distance), consists of finding the flight time t_f and the initial values of the adjoint variables $\{\lambda_r,\, \lambda_\theta,\, \lambda_u,\, \lambda_h\}$ that meet the four final conditions given by Eq. (6) and the transversality condition $\mathcal{H}(t_f) = 1$ [20]. When the path inequality constraint $r \geq r_{\min}$ is introduced in the optimization process, a switching structure is assumed a priori [20] and the following conditions are enforced at the (unknown) time instant $t_1 \in (t_0,\, t_f)$ [21]

$$r(t_1) = r_{\min} \quad , \quad u(t_1) = 0 \tag{11}$$

Accordingly, λ_r undergoes an "impulsive" variation (equal to $\Delta\lambda_{r_1}$) at t_1, while the other adjoint variables are all continuous. This result is consistent with Eq. (3.13.4) of Ref. [20], which describes the corner conditions of an optimal problem with state variable inequality constraints. In this case, the optimal transfer requires the solution of a three-point boundary value problem (3PBVP) in which the unknowns are the initial values of $\{\lambda_r,\, \lambda_\theta,\, \lambda_u,\, \lambda_h\}$, the variation $\Delta\lambda_{r_1}$, and the two time instants $\{t_1,\, t_f\}$, whereas the seven scalar constraints are $\mathcal{H}(t_f) = 1$ and those given by Eqs. (6) and (11). Finally, note that the optimal problem can be made independent of the initial heliostationary distance r_0 and the Sun's gravitational parameter $\mu_\odot$ by introducing a set of canonical units [22], in which the distance unit is r_0 and the time unit is $\sqrt{r_0^3/\mu_\odot}$. The numerical results and the analytical expressions discussed in the following sections are therefore general, in that they may be applied to a generic value of the design parameter r_0.

Numerical simulations

The optimization problem discussed in the previous section has been solved to simulate the optimal heliostationary-to-heliostationary transfer as a function of $\theta_f \in (0,\, \pi]\,\text{rad}$ and $r_{\min} \in \{0.3,\, 0.35,\, 0.4\}\, r_0$. Note that, assuming $r_0 = 1\,\text{au}$, the minimum Sun-spacecraft distance of $r_{\min} = 0.3\, r_0$ roughly corresponds to Mercury's perihelion radius. From a numerical viewpoint, Eqs. (4) and (8) have been integrated in double precision using a variable order Adams-Bashforth-Moulton solver [23, 24] with absolute and relative errors of 10^{-12}. The boundary-value problem has been solved by means of a hybrid numerical technique that combines genetic algorithms (to obtain a rough estimate of the adjoint variables) with gradient-based and direct methods (to refine the final solution).

Figure 2 shows the minimum dimensionless flight time t_f as a function of θ_f for the three values of $r_{\min}/r_0$ considered in the study. In particular, the three curves in Fig. 2 overlap when $\theta_f < 120\,\text{deg}$ because the constraint on the minimum Sun-spacecraft distance is inactive and, accordingly, the optimal transfer trajectory coincides with the solution of the corresponding 2PBVP. This aspect is confirmed by Fig. 3, which shows the dimensionless sail perihelion distance during the transfer as a function of the two design parameters $\{\theta_f, r_{\min}\}$.

An interesting and counterintuitive result, which emerges from Fig. 2, is the flight time variation with θ_f for a given value of the ratio $r_{\min}/r_0$. In fact, the function $t_f = t_f(\theta_f)$ reaches its maximum value when $\theta_f \to 0^+$, that is, the flight time tends to increase as the displacement angle θ_f decreases. This behaviour is better explained with the aid of Fig. 4 , which shows the maximum cone angle (Fig. 4(a)) and the maximum radial deviation (Fig. 4(b)) compared to the initial solar distance as a function of $\theta_f \in (0,\, 30]\,\text{deg}$. As long as the displacement angle θ_f is sufficiently small, during the transfer the optimal cone angle is close to the value $\alpha = 0$ required to maintain the heliostationary condition. Therefore, the transverse component of the propulsive acceleration vector, which scales with $\sin\alpha$ [see the second of Eqs. (3)], is very small during all of the transfer and this fact increases the flight time. Moreover, Fig. 4(b) shows that, when θ_f is small, the Sun-spacecraft distance remains close to its initial value r_0. In other terms, the numerical simulations indicate that the approximations

$$r \simeq r_0 \;\cap\; \alpha \ll 1 \quad \text{for} \quad t \in [t_0,\, t_f] \tag{12}$$

are consistent with the actual behaviour of the optimal transfer trajectory as long as $\theta_f \ll 1$. These approximations form the foundation for the analytical result discussed in the next section.

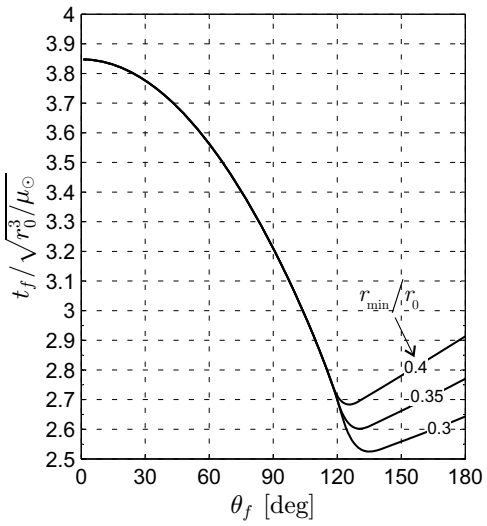

Figure 2 Minimum dimensionless flight time as a function of θ_f and $r_{\min}/r_0$.

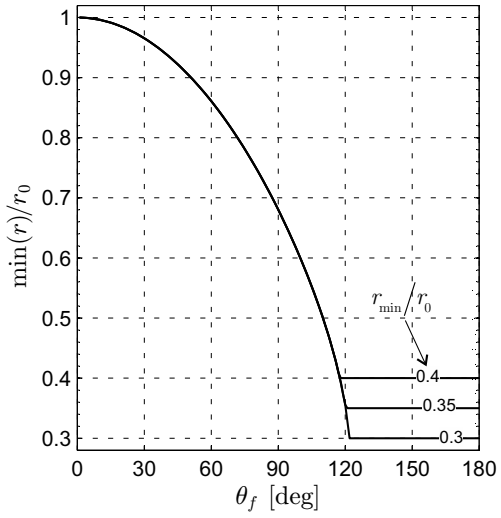

Figure 3 Dimensionless perihelion distance as a function of θ_f and $r_{\min}/r_0$.

Analytical approximation for small displacement angles

When the displacement angle θ_f is sufficiently small, the optimization problem is simplified by the introduction of the approximations given by Eq. (12). Indeed, using the fact that $\cos^2\alpha\,\sin\alpha \simeq \alpha$ and $(1-\cos^3\alpha) \simeq 3\alpha^2/2$, the last three equations of motion (4) reduce to

$$\dot{\theta} = \frac{h}{r_0^2} \tag{13}$$

$$\dot{u} = \frac{h^2}{r_0^3} - \frac{3\,\mu_\odot}{2\,r_0^2}\,\alpha^2 \tag{14}$$

$$\dot{h} = \frac{\mu_\odot}{r_0}\,\alpha \tag{15}$$

with initial conditions still given by the last three Eqs. (5). Using again an indirect approach to solve the optimization problem, the Hamiltonian function now becomes

$$\mathcal{H} = \lambda_\theta\,\frac{h}{r_0^2} + \lambda_u\,\frac{h^2}{r_0^3} + \frac{\mu_\odot}{r_0}\,\mathcal{F} \tag{16}$$

where $\mathcal{F} = \mathcal{F}(\lambda_u, \lambda_h, \alpha)$ is an auxiliary function, given by

$$\mathcal{F} \triangleq \lambda_h\,\alpha - \frac{3\,\lambda_u}{2\,r_0}\,\alpha^2 \tag{17}$$

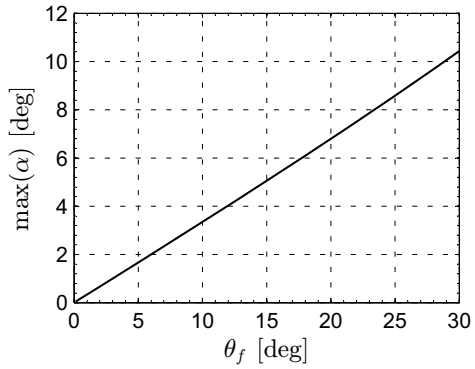

a) $\max(\alpha)$.

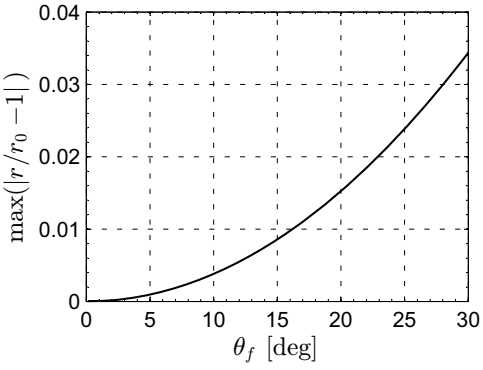

b) $\max(|r/r_0 - 1|)$.

Figure 4 Maximum cone angle and maximum radial deviation as a function of θ_f.

and the Euler-Lagrange equations are

$$\dot{\lambda}_\theta = 0 \tag{18}$$

$$\dot{\lambda}_u = 0 \tag{19}$$

$$\dot{\lambda}_h = -\frac{\lambda_\theta}{r_0^2} - \frac{2\,\lambda_u\,h}{r_0^3} \tag{20}$$

In this (approximate) case, λ_θ and λ_u are both constants of motion, while λ_h is a time-varying function with

$$\lambda_h(t_0) = \lambda_{h_0} \quad , \quad \dot{\lambda}_h(t_0) = -\frac{\lambda_\theta}{r_0^2} \tag{21}$$

where λ_{h_0} is a parameter to be found as a part of the general solution, whereas the second of Eqs. (21) is a consequence of the initial condition $h(t_0) = 0$; see Eq. (5).

The optimal cone angle is obtained by maximizing $\mathcal{F}$ with respect to α in Eq. (17). Since λ_u is a constant of motion and $\mathcal{F}$ is a quadratic function of α, the maximization of $\mathcal{F}$ corresponds to either $\alpha = 0$ or $\alpha = \pi/2\,\mathrm{rad}$ along the whole transfer if $\lambda_u \leq 0$. The latter condition on λ_u is however unfeasible, since if $\alpha = 0$, the spacecraft remains in its initial position, whereas if $\alpha = \pi/2\,\mathrm{rad}$, the propulsive acceleration goes to zero and the spacecraft falls toward the Sun along a rectilinear trajectory [25–27]. Assuming therefore $\lambda_u > 0$, the cone angle that maximizes $\mathcal{F}$ is

$$\alpha = \frac{\lambda_h\,r_0}{3\,\lambda_u} \tag{22}$$

The adjoint variable λ_u can be written as a function of λ_{h_0} by exploiting the transversality condition $\mathcal{H}(t_f) = 1$ [20]. In fact, because the Hamiltonian function is again a constant of motion [18], the transversality condition can be equivalently rewritten as $\mathcal{H}(t_0) = 1$. The latter, with the aid of Eqs. (5), (16)-(17) and (22), gives

$$\lambda_u = \frac{\mu_\odot\,\lambda_{h_0}^2}{6} \tag{23}$$

The expression of λ_h is obtained by taking the time derivative of Eq. (20). More precisely, bearing in mind Eqs. (15), (18)-(19), and (22), it may be verified that

$$\ddot{\lambda}_h + \omega^2\,\lambda_h = 0 \qquad \text{with} \qquad \omega \triangleq \sqrt{\frac{2\,\mu_\odot}{3\,r_0^3}} \tag{24}$$

Using the initial conditions (21), the time variation of λ_h may be written as a function of the unknown parameters $\{\lambda_{h_0},\, \lambda_\theta\}$ as

$$\lambda_h = \lambda_{h_0}\, \cos(\omega\, t) - \frac{\lambda_\theta}{\omega\, r_0^2}\, \sin(\omega\, t) \tag{25}$$

The optimal time variation of α is then obtained substituting Eqs. (23) and (25) into (22). The result is

$$\alpha = \frac{2\, r_0}{\mu_\odot\, \lambda_{h_0}}\, \cos(\omega\, t) - \frac{2\, \lambda_\theta}{\mu_\odot\, \omega\, r_0\, \lambda_{h_0}^2}\, \sin(\omega\, t) \tag{26}$$

The latter may be substituted into Eq. (15) to obtain, after integration, the expression of the specific angular momentum magnitude as

$$h = \frac{2}{\lambda_{h_0}\, \omega}\, \sin(\omega\, t) - \frac{4\, \lambda_\theta}{\lambda_{h_0}^2\, \omega^2\, r_0^2}\, \sin^2\left(\frac{\omega\, t}{2}\right) \tag{27}$$

Then, Eqs. (13) and (27) give the time variation of the polar angle

$$\theta = \frac{2\, \lambda_\theta}{\lambda_{h_0}^2\, \omega^3\, r_0^4}\, \sin(\omega\, t) + \frac{4}{\lambda_{h_0}\, \omega^2\, r_0^2}\, \sin^2\left(\frac{\omega\, t}{2}\right) - \frac{2\, \lambda_\theta}{\lambda_{h_0}^2\, \omega^2\, r_0^4}\, t \tag{28}$$

and Eqs. (14) and (26)-(27) provide the expression of u as

$$u = \frac{8\lambda_{h_0}\lambda_\theta\omega r_0^2\cos(\omega\, t)\, [1-\cos(\omega\, t)] - 8\lambda_\theta^2\sin(\omega\, t) - \left(2\lambda_{h_0}^2\omega^2 r_0^4 - 2\lambda_\theta^2\right)\sin(2\omega\, t) + 4\lambda_\theta^2\omega\, t}{\lambda_{h_0}^4\, \omega^5\, r_0^7} \tag{29}$$

Note that Eqs. (27)–(29) give the time variation of the spacecraft states $\{h,\, \theta,\, u\}$ as a function of $\{\lambda_{h_0},\, \lambda_\theta\}$. In particular, Eq. (28) (or Eq. (29)) contains a secular term proportional to λ_θ (or λ_θ^2), while h is a periodic function of time.

The values of $\{\lambda_{h_0}, \lambda_\theta\}$ and the minimum flight time t_f are obtained by enforcing the terminal conditions (6) into Eqs. (27)–(29). The result is the closed form solution of the (simplified) optimization problem, or

$$\lambda_{h_0} = \frac{6\, r_0}{\mu_\odot\, \theta_f} \quad , \quad \lambda_\theta = 0 \quad , \quad t_f = \frac{\pi}{\omega} \equiv \pi\sqrt{\frac{3\, r_0^3}{2\, \mu_\odot}} \tag{30}$$

In addition, Eq. (23) gives λ_u as a function of the mission parameters

$$\lambda_u = \frac{6\, r_0^2}{\mu_\odot\, \theta_f^2} \tag{31}$$

and Eqs. (27)–(30) provide the analytical approximations of the optimal transfer trajectory in terms of time-histories of the state variables, viz.

$$\theta = \theta_f\, \sin^2\left(\frac{\omega\, t}{2}\right) \tag{32}$$

$$u = -\frac{\omega\, r_0\, \theta_f^2}{8}\, \sin(2\, \omega\, t) \tag{33}$$

$$h = \frac{\omega\, r_0^2\, \theta_f}{2}\, \sin(\omega\, t) \tag{34}$$

from which it is clear that the analytical approximation of the state variables comply with the initial boundary conditions (5) at $t_0 = 0$ and with the final boundary conditions (6) at $t_f = \pi/\omega$. Finally, Eq. (26) gives the time variation of the optimal cone angle as

$$\alpha = \frac{\theta_f}{3}\, \cos(\omega\, t) \tag{35}$$

that is, the maximum value of α is proportional to θ_f. In other terms, as long as θ_f is small, during the transfer the sail cone angle is nearly zero, in accordance with Fig. 4(a).

Some remarks on the approximate analytical model are in order: 1) strictly speaking, Eqs. (32)–(35) are valid for $t \in [t_0,\, t_f]$, that is, for $t \in [0,\, \pi/\omega]$; 2) the maximum value of u is small as it is proportional to θ_f^2 (this is consistent with the assumption of $r \simeq r_0$); 3) the minimum flight time t_f is independent of the target polar angle θ_f, see Eq. (30). The latter is a consequence of the assumption of a small value of θ_f, which, in its turn, is at the basis of the approximations (12). In fact, the function $t_f = t_f(\theta_f)$ is nearly constant within the range $0 < \theta_f \leq 30\,\text{deg}$, see Fig. 2, and $t_f/\sqrt{r_0^3/\mu_\odot} \simeq 3.847$ as $\theta_f \to 0^+$. Notably, the latter result on the flight time is accurately approximated by Eq. (30), according to which $t_f/\sqrt{r_0^3/\mu_\odot} \simeq \pi\sqrt{3/2} \simeq 3.847$. A further analysis of Eqs. (32)–(34) highlights the influence of θ_f on the time histories of $\{\theta, u, h, \alpha\}$. In particular, the final polar angle only affects the peak value of the state variable oscillations without changing their frequencies, which only depend on the initial Sun-spacecraft distance r_0 through ω; see Eq. (24).

To validate the approximation $r(t) \simeq r_0$, the function $r(t)$ obtained numerically is now compared with the analytical result that comes from the integration of the radial velocity u given by Eq. (33), or

$$r(t) = r_0 - \frac{r_0\, \theta_f^2}{16}\, [1 - \cos(2\, \omega\, t)] \tag{36}$$

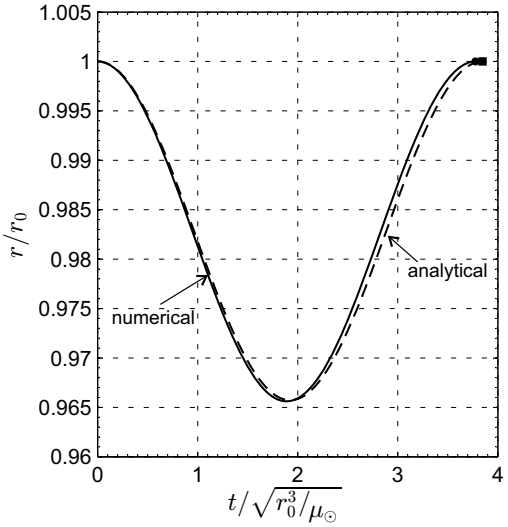

a) $\theta_f = 30\,\text{deg}$.

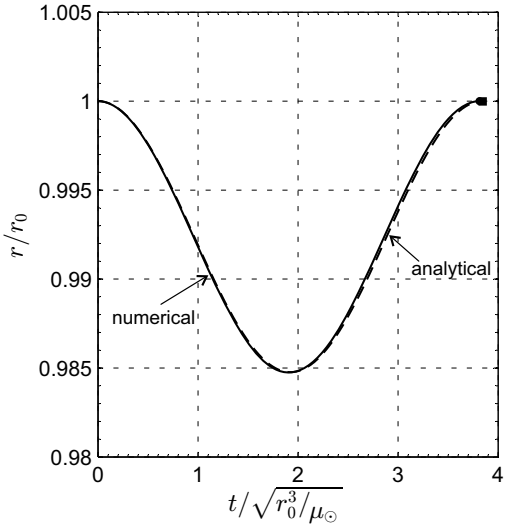

b) $\theta_f = 20\,\text{deg}$.

Figure 5 Comparison between numerical solution (solid line) and analytical approximation (dashed line) of $r = r(t)$ for $\theta_f = \{20,\ 30\}$ deg.

Figure 5 shows that when $\theta_f = 30\,\text{deg}$, the analytical approximation of $r(t)$ is close to its numerical value, with a maximum error, defined as $|1 - r(t)/r_0|$, of about 3.5%. When θ_f is decreased to 20 deg, the analytical and numerical time histories of $r(t)$ are nearly coincident, with a maximum error less than 1.6%. These results confirm the soundness of the assumption $r(t) \simeq r_0$ during the transfer. The accuracy of the analytical approximations (32)–(34) is better appreciated with the aid of Fig. 6, which shows the time variation of $\{\theta, u, h\}$ in an optimal transfer when $\theta_f = \{20, 30\}$ deg. The analytical method also provides a good approximation of the actual optimal control law $\alpha = \alpha(t)$. This is apparent in Fig. 7, which compares the numerical optimal value of $\alpha(t)$ with the sinusoidal approximation given by Eq. (35).

The accuracy of Eq. (35) allows the designer to obtain a reference steering law that is able to estimate the actual nonlinear behaviour of the sail during the optimal transfer. In fact, when the system dynamics are simulated by integrating its equations of motion (4), but using the control law $\alpha(t)$ taken from Eq. (35), the spacecraft closely approaches the desired target conditions given by Eqs. (6). To quantify this result, let $\mathcal{E}_i$ be the dimensionless error associated with an estimate of the generic state variable $i = \{r,\, \theta,\, u,\, h\}$, calculated at $t_f = \pi/\omega$, and obtained by integrating the nonlinear equations of motion (4) with the analytical steering law of Eq. (35). For example, $\mathcal{E}_r = r(t_f)/r_0 - 1$, while $\mathcal{E}_u = u(t_f)/\sqrt{\mu_\odot/r_0}$ when $t_f = \pi/\omega$. Figure 8 shows the dimensionless errors $\mathcal{E}_i$ as functions of θ_f. Not only tend all errors to zero for small values of θ_f, but they remain small even for large values of θ_f. Finally, Fig. 9 compares the approximate flight time $t_f = \pi/\omega$ with that calculated numerically. Again, the results confirm the accuracy of the approximation.

The analytical model provides a set of initial guesses for a solution of the 2PBVP that uses the original (nonlinear) equations of motion (4). In particular, Eqs. (30)-(31) may be used to estimate the initial value of the adjoint variables $\{\lambda_\theta, \lambda_u, \lambda_h\}$, which simplifies the convergence of the numerical algorithms towards the final solution. This aspect of the optimization process is confirmed by Table 1, where the actual values of the initial adjoint variables (in canonical units) are compared with those obtained through the analytical approximate model. Note the different order of magnitude between $\{\lambda_h(t_0), \lambda_u(t_0)\}$ and λ_θ when $\theta_f \ll 1$.

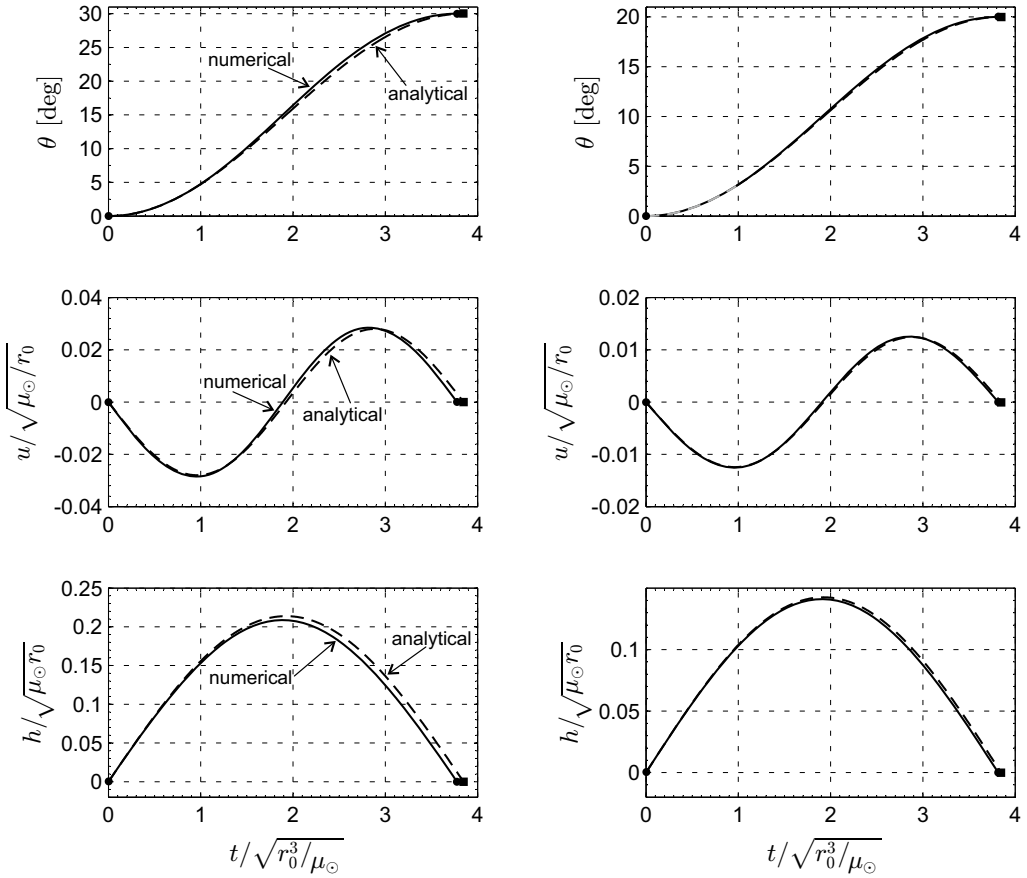

a) $\theta_f = 30\,\text{deg}$. **b)** $\theta_f = 20\,\text{deg}$.

Figure 6 Time variation of the state variables: comparison between numerical solution (solid line) and analytical approximation (dashed line).

Table 1 Accuracy in guessing the initial value of the unknown adjoint variables $\{\lambda_\theta, \lambda_u, \lambda_h\}$ (in canonical units).

θ_f [deg]	model	λ_θ	$\lambda_u(t_0)$	$\lambda_h(t_0)$
5	numerical	−0.0455	784.0478	68.6388
	analytical	0	787.8735	68.7549
20	numerical	−0.1818	45.4587	16.7255
	analytical	0	49.2421	17.1887
30	numerical	−0.2727	18.1578	10.7668
	analytical	0	21.8854	11.4592
45	numerical	−0.4084	6.1233	6.6094
	analytical	0	9.7268	7.6394

Conclusions

The results discussed in this Note allow a designer to get a rapid estimation of the time-optimal trajectory of a high-performance solar sail in a transfer between heliostationary points. The analytical model, which is valid under the assumption of short distance between the initial and the final heliostationary positions, gives a useful and accurate approximation of the optimal control law, which can be used as an initial guess to drive the system towards the target state in a real (nonlinear) mission scenario.

The existence of a closed-form solution is an uncommon result in optimal control problems and may be therefore considered as a favourable event. In addition, such a solution is useful for accurate initial guesses of the adjoint variables, which guarantee a fast numerical convergence of the original nonlinear problem.

Acknowledgments

This work is supported by the University of Pisa, Progetti di Ricerca di Ateneo (Grant no. PRA-2018-44).

References

[1] Fu, B., Sperber, E., and Eke, F., "Solar sail technology–A state of the art review," *Progress in Aerospace Sciences*, Vol. 86, October 2016, pp. 1–19. doi: https://doi.org/10.1016/j.paerosci.2016.07.001.

[2] Gong, S. and Macdonald, M., "Review on solar sail technology," *Astrodynamics*, Vol. 3, No. 2, June 2019, pp. 93–125. doi: https://doi.org/10.1007/s42064-019-0038-x.

[3] Dachwald, B., Seboldt, W., Macdonald, M., Mengali, G., Quarta, A. A., McInnes, C. R., Rios-Reyes, L., Scheers, D., Wie, B., Görlich, M., Lura, F., Diedrich, B., Baturkin, V., Coverstone, V., Leipold, M., and Garbe, G., "Potential Solar Sail Degradation Effects on Trajectory and Attitude Control," *AIAA Guidance, Navigation, and Control Conference and Exhibit*, San Francisco, USA, 15–18 August 2005, Paper AIAA 2005-6172. doi: https://doi.org/10.2514/6.2005-6172.

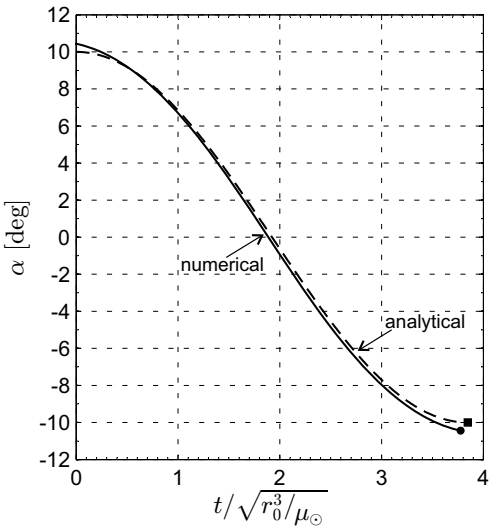

a) $\theta_f = 30\,\text{deg}$.

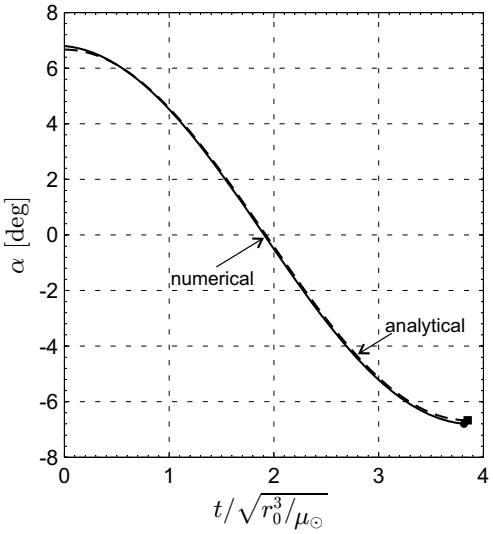

b) $\theta_f = 20\,\text{deg}$.

Figure 7 Time variation of the optimal cone angle: comparison between numerical (solid line) and analytical approximation (dashed line).

[4] Dachwald, B., Mengali, G., Quarta, A. A., and Macdonald, M., "Parametric model and optimal control of solar sails with optical degradation," *Journal of Guidance, Control, and Dynamics*, Vol. 29, No. 5, September-October 2006, pp. 1170–1178. doi: https://doi.org/10.2514/1.20313.

[5] McInnes, C. R., "Approximate Closed-Form Solution for Solar Sail Spiral Trajectories with Sail Degradation," *Journal of Guidance, Control, and Dynamics*, Vol. 37, No. 6, 2014, pp. 2053–2057. doi: https://doi.org/10.2514/1.G000225.

[6] McKay, R. J., Macdonald, M., Biggs, J. D., and McInnes, C. R., "Survey of Highly Non-Keplerian Orbits with Low-Thrust Propulsion," *Journal of Guidance, Control, and Dynamics*, Vol. 34, No. 3, 2011, pp. 645–666. doi: https://doi.org/10.2514/1.52133.

[7] Montgomery, E., Heaton, A., and Garbe, G., "Places Only Solar Sails Can Go," *AIAA International Air and Space Symposium and Exposition: The Next 100 Years*, Dayton, Ohio, July 2003, Paper AIAA 2003-2836. doi: https://doi.org/10.2514/6.2003-2836.

[8] Macdonald, M. and McInnes, C. R., "Solar sail science mission applications and advancement," *Advances in Space Research*, Vol. 48, No. 11, Dec. 2011, pp. 1702–1716. doi: https://doi.org/10.1016/j.asr.2011.03.018.

[9] McInnes, C. R., "Inverse Solar Sail Trajectory Problem," *Journal of Guidance, Control, and Dynamics*, Vol. 26, No. 2, 2003, pp. 369–371. doi: https://doi.org/10.2514/2.5057.

[10] Mengali, G. and Quarta, A. A., "Optimal heliostationary missions of high-performance sailcraft," *Acta Astronautica*, Vol. 60, No. 8-9, April-May 2007, pp. 676–683. doi: https://doi.org/10.1016/j.actaastro.2006.07.018.

[11] McInnes, C. R., *Solar Sailing: Technology, Dynamics and Mission Applications*, chap. 2, Springer-Verlag Berlin, 1999, pp. 47–51, ISBN: 978-1-85233-102-3.

[12] Vulpetti, G., *Fast Solar Sailing: Astrodynamics of Special Sailcraft Trajectories*, chap. 7, Springer Netherlands, 2013, pp. 274–295, ISBN:978-94-007-4776-0.

[13] Sauer, Jr., C. G., "Solar Sail Trajectories for Solar Polar and Interstellar Probe Missions," *AAS/AIAA Astrodynamics Specialist Conference*, Girdwood, Alaska, 1999, Paper AAS 99-336.

[14] Dandouras, I., Pirard, B., and Prado, J. Y., "High Performance Solar Sails for Linear Trajectories and Heliostationary Missions," *Advances in Space Research*, Vol. 34, No. 1, 2004, pp. 198–203. doi: https://doi.org/10.1016/j.asr.2003.02.055.

[15] Bassetto, M., Mengali, G., and Quarta, A. A., "Stability and Control of Spinning E-sail in Heliostationary Orbit," *Journal of Guidance, Control, and Dynamics*, Vol. 42, Feb. 2019, pp. 425–431. doi: https://doi.org/10.2514/1.G003788.

[16] Wright, J. L., *Space Sailing*, Gordon and Breach Science Publishers , 1992, pp. 223–233, ISBN: 978-2881248030.

[17] Mengali, G., Quarta, A. A., Circi, C., and Dachwald, B., "Refined solar sail force model with mission application," *Journal of Guidance, Control, and Dynamics*, Vol. 30, No. 2, March-April 2007, pp. 512–520. doi: https://doi.org/10.2514/1.24779.

[18] Stengel, R. F., *Optimal Control and Estimation*, Dover Publications, Mineola, NY, 1994, pp. 222–254, ISBN: 978-0486682006.

[19] Sauer, C. G., "Optimum solar-sail interplanetary trajectories," *AIAA/AAS Astrodynamics Conference*, San Diego (CA), Aug. 1976, Paper AIAA 76-792. doi: https://doi.org/10.2514/6.1976-792.

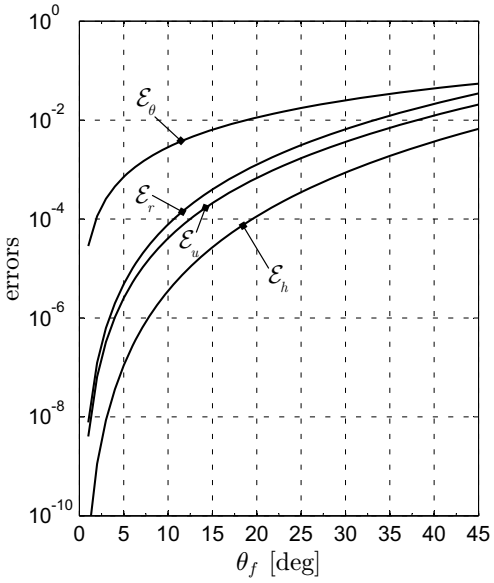

Figure 8 Dimensionless difference between target state and actual state (at $t_f = \pi/\omega$) obtained by integrating Eqs. (4) with the analytical control law of Eq. (35) .

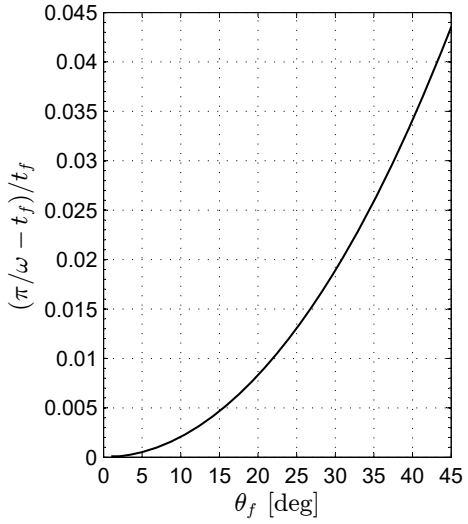

Figure 9 Dimensionless relative error of the analytical approximation in estimating the flight time as a function of θ_f. The value of t_f refers to the minimum flight time obtained by numerical approach.

[20] Bryson, A. E. and Ho, Y. C., *Applied Optimal Control*, chap. 1, Hemisphere Publishing Corporation, New York, NY, 1975, pp. 9–18, ISBN: 0-891-16228-3.

[21] Quarta, A. A. and Mengali, G., "Electric Sail Mission Analysis for Outer Solar System Exploration," *Journal of Guidance, Control, and Dynamics*, Vol. 33, No. 3, May-June 2010, pp. 740–755. doi: https://doi.org/10.2514/1.47006.

[22] Bate, R. R., Mueller, D. D., and White, J. E., *Fundamentals of Astrodynamics*, Dover Publications, New York, 1971, p. 429, ISBN: 978-0486600611.

[23] Shampine, L. F. and Gordon, M. K., *Computer Solution of Ordinary Differential Equations: The Initial Value Problem*, chap. 10, W. H. Freeman, San Francisco, 1975, ISBN: 978-0716704614.

[24] Shampine, L. F. and Reichelt, M. W., "The MATLAB ODE Suite," *SIAM Journal on Scientific Computing*, Vol. 18, No. 1, January 1997, pp. 1–22. doi: https://doi.org/10.1137/S1064827594276424.

[25] Quarta, A. A. and Mengali, G., "Solar Sail Capabilities to Reach Elliptic Rectilinear Orbits," *Journal of Guidance, Control, and Dynamics*, Vol. 34, No. 3, May-June 2011, pp. 923–926. doi: https://doi.org/10.2514/1.51638.

[26] Quarta, A. A. and Mengali, G., "Optimal Solar Sail Transfer to Linear Trajectories," *Acta Astronautica*, Vol. 82, No. 2, February 2013, pp. 189–196. doi: https://doi.org/10.1016/j.actaastro.2012.03.005.

[27] Quarta, A. A., Mengali, G., and Caruso, A., "Optimal Circle-to-Rectilinear Orbit Transfer with Circumferential Thrust," *Astrodynamics*, Vol. 3, No. 1, March 2019, pp. 31–43. doi: https://doi.org/10.1007/s42064-018-0034-9.